Mendeleev Communications

Mendeleev Commun., 2025, **35**, 320–323

Multiscale simulation of spectroscopic properties of B3PYMPM–CBP exciplexes in OLEDs

Nikita O. Dubinets*[a,b,c] and Alexandra Ya. Freidzon[a,d]

[a] *National Research Nuclear University MEPhI, 115409 Moscow, Russian Federation. E-mail: nikita.dubinets@gmail.com*
[b] *N. S. Enikolopov Institute of Synthetic Polymeric Materials, Russian Academy of Sciences, 117393 Moscow, Russian Federation*
[c] *National Research Center 'Kurchatov Institute', 119421 Moscow, Russian Federation*
[d] *Weizmann Institute of Science, 7610001 Rehovot, Israel*

DOI: 10.71267/mencom.7635

Using polarizable continuum model, QM/MM and effective fragment potential (EFP) approaches, exciplex luminescence at the interface of two organic semiconductors, electron transporter B3PYMPM and hole transporter CBP, was simulated taking into account their environment. The effects of multiple nonequilibrium molecular conformations in the sample and the polarizable environment of the chromophores were analyzed. It was found that EFP provides the best description of the environment, making it possible to include both structural effects and molecular polarizability.

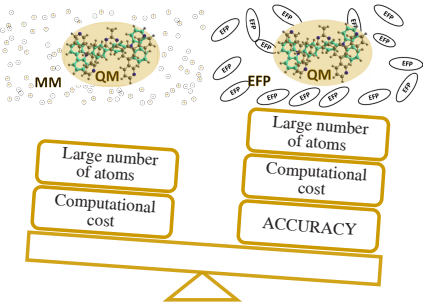

Keywords: exciplex, OLED, interface, DFT, QM/MM, QM/EFP.

Exciplexes in blends or at the interfaces of donor and acceptor organic semiconductors are rather common.[1–3] In first-generation (fluorescence-based) organic light-emitting diodes (OLEDs), the formation of weakly emitting exciplexes is considered a factor that worsens their emission efficiency and color purity.[4,5] The use of exciplexes in OLEDs can lead to simplification of the device architecture, reduction of driving voltages, improvement of outcoupling, increase in power efficiency and the possibility of producing white-light OLEDs with a spectrum close to daylight.[6–8]

The molecular mechanical treatment of the environment within the quantum mechanics/molecular mechanics (QM/MM) framework [Figure S1(*a*), see Online Supplementary Materials] seems to be rather promising, especially when using polarizable force fields. However, the molecular mechanical approach depends on the parameterization of the force field.[9–11] The effective fragment potential (EFP)[12,13] is a potential generated *ab initio* [Figure S1(*b*)] in which the total intermolecular interaction energy of the system is represented as a sum of electrostatic (coulombic), polarization (induction), dispersion, exchange repulsion and charge transfer energies. One of the advantages of the EFP method is the possibility of partitioning large molecules of the environment into smaller fragments,[14] generating potential parameters for them and constructing the total potential of the environment from the fragment potentials.[15] Using EFP for a polarizable environment is a reasonable trade-off between accuracy and computational costs.

In this work, we investigated the formation of exciplexes between the electron-deficient material B3PYMPM and the fluorophore CBP using a multiscale approach combining molecular dynamics (MD) and quantum chemistry (QC) calculations. Different levels of environment treatment were tested to obtain the most reliable description of the interfacial exciplexes.

The aim of this work was to develop a computational procedure for simulating the spectra of donor–acceptor complexes taking into account their environment. We calculated the absorption, fluorescence and phosphorescence spectra of individual CBP and B3PYMPM in bulk and their blend and analyzed the effects arising from nonequilibrium conformations of the molecules and their inhomogeneous environment in amorphous solids.

Figure 1 shows the optimized structures of B3PYMPM and CBP. The geometry of each molecule was optimized in the ground and excited states using DFT or TD-DFT with BHHLYP functional[16] and def2-SVP basis set.[17] The D3BJ dispersion correction was used. In these geometries, the vertical energies of excitation, emission, electron attachment and detachment were calculated (Table S1, see Online Supplementary Materials) at the same level of theory with the def2-TZVP basis set.[18] Note that for fluorescence we used only the $S_1 \rightarrow S_0$ transition and for phosphorescence the $T_1 \rightarrow S_0$ transition. The BHHLYP functional was chosen since it has 50% HF exchange and successfully excludes artifactual charge-transfer states, albeit at the cost of a slight overestimation of the energies of local transitions.[8] The calculations were performed using the ORCA[19,20] and GAMESS (US)[21] packages.

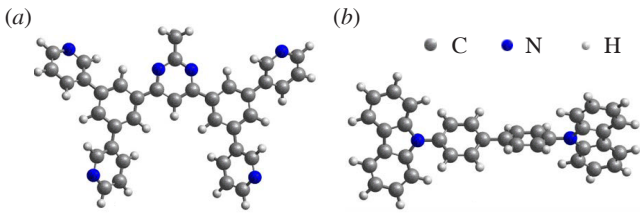

Figure 1 Optimized structures of (*a*) B3PYMPM and (*b*) CBP.

MD simulations of individual bulk amorphous B3PYMPM and CBP layers were then performed using the GROMACS package[22] in the OPLS-aa force field.[23,24] Tetragonal cells of 10 × 10 × 5 nm (Figure S2) were constructed from 396 B3PYMPM molecules or 455 CBP molecules. Each cell was optimized and NPT relaxation was performed at 600 K to achieve realistic density, after which 100 000 2-fs steps were run at room temperature.

The cells were then merged along the *z*-axis to create a 10 × 10 × 10 nm cubic cell (Figure 2) and the MD simulation was run again. The energy of the merged cell was minimized and an NPT relaxation of 250 000 2-fs steps was performed at room temperature.

To search for contact pairs at the interface, we took molecules in which at least one of the distances between two nitrogen atoms of CBP and three carbon atoms of B3PYMPM was less than 5.6 Å (Figure S3). As a result, 20 exciplex pairs of CBP and B3PYMPM were found (Figure S4).

The binding energy of the exciplex in the ground state is calculated by the equation:

$$E_b(S_0) = E_{B3PYMPM}(S_0) + E_{CBP}(S_0) - E_{B3PYMPM–CBP}(S_0).$$

The binding energy of the exciplex in the excited state can be determined in two ways. The binding energy of the donor cation and acceptor anion, defined as

$$E_b^1(S_1) = E_{B3PYMPM^-} + E_{CBP^+} - E_{B3PYMPM–CBP}(S_1),$$

is used when considering the dissociation of the charge transfer state. The binding energy of electronically excited monomers from the equation

$$E_b^2(S_1) = E_{CBP}(S_1) + E_{B3PYMPM}(S_0) - E_{B3PYMPM–CBP}(S_1)$$

is used to assess the possibility of exciplex formation from excited monomers. Table S2 lists the binding energies for the gas phase and the polarizable continuum model (PCM) only. In QM/MM calculations, no common origin of energy can be properly identified: each individual monomer molecule exists in its own environment, and therefore the QM/MM energies of the monomers cannot serve as the energy origin.

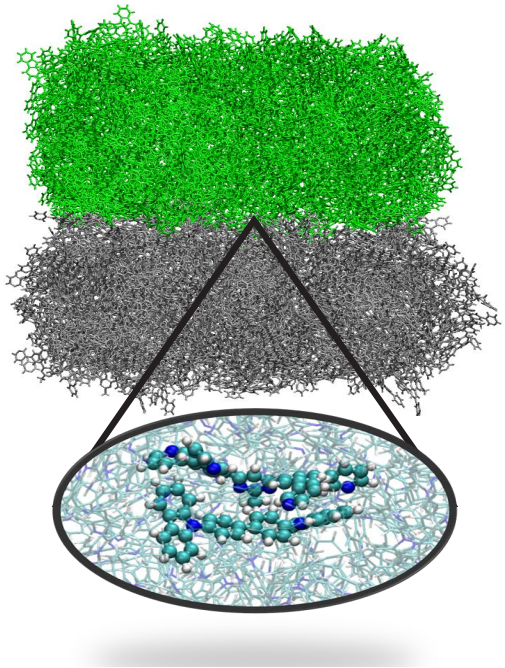

Figure 2 A merged cubic cell containing the B3PYMPM–CBP interface.

The positive binding energy $E_b^2(S_1)$ means that exciplexes are indeed formed upon excitation of B3PYMPM. The positive binding energy $E_b^1(S_1)$ means that the corresponding exciplexes are stable against dissociation into cation and anion. Table S2 shows that for all CBP–B3PYMPM complexes in the gas phase, the binding energy is much higher in the excited state than in the ground state. Solvation can either decrease or slightly increase the binding energy in the excited state compared to the gas phase and definitely decrease the binding energy in the ground state, so that in some cases it becomes negative.

Electron density analysis (Figure S5) shows that the CBP–B3PYMPM exciplex is formed with charge transfer from CBP to B3PYMPM, making this system useful in organic light-emitting devices. In about 20% of the complexes, the S_1 state was localized on CBP, which is confirmed by the data in Figure S6: the $S_0 \rightarrow S_1$ transition has a shorter wavelength, higher oscillator strength and low or negative binding energies.

The absorption, fluorescence and phosphorescence spectra were calculated using BHHLYP/def2-TZVP with geometries optimized by the following methods. The ground and excited states in the gas phase were optimized with further calculation of the spectra either (i) *in vacuo* or (ii) with implicit solvation *via* PCM ($\varepsilon = 3^{\dagger}$). (iii) The explicit environment included *via* QM/MM was considered by cutting out the molecules surrounding each pair in the MD cell at a radius of 7 Å. The geometry of each pair was optimized by additive QM/MM with electrostatic embedding at the same level of theory as above. The pairs of interest representing the QM part and the environment constituting the MM part were frozen. (iv) Finally, QM/EFP calculations were performed using the structures optimized by QM/MM. For this purpose, each molecule of the environment (CBP or B3PYMPM) was represented by a set of EFPs (Figure S7). CBP was partitioned into two benzene and two carbazole fragments, and B3PYMPM was partitioned into two benzene, four pyridine and one pyrazine fragments.

For each fragment, the EFP parameters were calculated (Figure S8). The fragments were then combined into real geometries according to a previously published procedure.[13] As a result, 20 geometries of exciplexes surrounded by EFPs were generated. For these structures, the binding energies of the exciplexes and their absorption ($S_0 \rightarrow S_n$), fluorescence ($S_1 \rightarrow S_0$) and phosphorescence ($T_1 \rightarrow S_0$) spectra were calculated.

In addition to the interface, bulk amorphous layers of individual B3PYMPM and CBP were considered using previously constructed tetragonal cells of 10 × 10 × 5 nm size from 396 B3PYMPM molecules and 455 CBP molecules, respectively. From these cells, 20 CBP and 20 B3PYMPM molecules were cut out together with their environment within a radius of 7 Å. Their absorption and emission spectra were calculated similarly to exciplexes in the gas phase, in PCM and at the QM/MM and QM/EFP level of theory.

Finally, to account for possible excitonic effects, we calculated the gas-phase absorption spectra of B3PYMPM and CBP dimers cut from the corresponding bulk amorphous layers. If excitonic interactions are present, the spectra should be red-shifted.

The broadened spectra were constructed as follows. The stick spectra of the $S_0 \rightarrow S_1$ electronic transitions in each pair or monomer (in the case of bulk B3PYMPM and CBP) were broadened by Gaussians with FWHM = 0.17 eV and summed up.

The above results show that the environment strongly affects the stability of the exciplexes and can even promote the flip of local and charge transfer states. Therefore, we plotted the absorption, fluorescence and phosphorescence spectra of the

[†] In weakly polar organic media, the value of static dielectric constant does not exceed 3.

complexes using different environment models. PCM includes only the homogeneous polarization of the environment, the employed QM/MM version includes only the relaxation of the environment, and the relaxed environment-based EFP includes the inhomogeneous polarization of the environment.

The calculated absorption spectra of B3PYMPM and CBP [Figure S9(*a*),(*b*)] consist of locally excited bands. The polarizable continuum environment only slightly affects the positions of the absorption maxima. The discrete environment causes a drastic distortion of the monomer structure, which leads to noticeable shifts of the absorption bands. The experimental absorption maximum of B3PYMPM is almost the same in the thin film and in the solution. The calculated spectra of B3PYMPM are in qualitative agreement with the experimental data. At the same time, the experimental absorption of CBP in the solid state is slightly red-shifted compared to the solution, which is also reproduced by our calculations. The calculated spectra of the dimers in the gas phase are not red-shifted relative to the spectra of the corresponding monomers and have almost the same shape. This indicates that there were no pairs with noticeable excitonic interactions in the dimer samples. Nevertheless, such interactions are possible in the case of sufficiently close packing of monomers, which is unlikely to be achieved in amorphous layers.

As for the complexes [Figure S9(*c*)], the charge transfer transitions should have zero intensity, while the intense local transitions should belong to CBP. This trend can be seen in the calculated gas-phase and PCM spectra of the complexes. However, the geometric distortions caused by the explicit environment and, more importantly, the charge distribution and polarizability of the environment not only make the charge transfer transition intensity noticeably non-zero, but also red-shift the local transition of CBP. As a result, the overall absorption of the complexes is red-shifted to 310–350 nm, which is consistent with the experimental absorption of solid CBP. In the absence of available absorption data for the co-deposited CBP–B3PYMPM films, we cannot directly compare this theoretical result with the experiment.

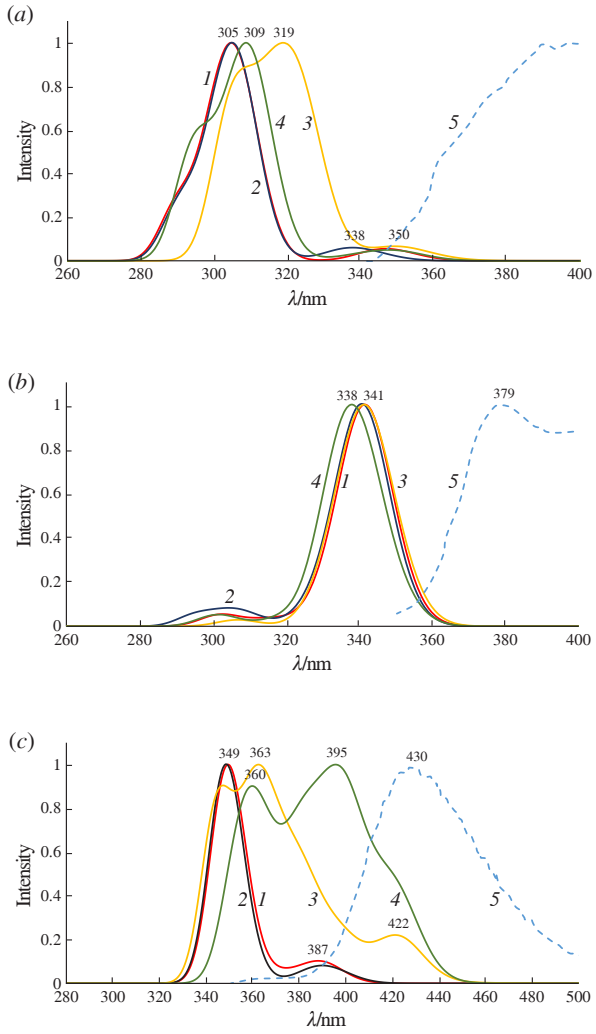

Figure 3 Fluorescence spectra of (*a*) B3PYMPM, (*b*) CBP and (*c*) CBP–B3PYMPM exciplexes calculated (*1*) in the gas phase, (*2*) in PCM and at (*3*) QM/MM and (*4*) QM/EFP levels of environment treatment in comparison with (*5*) the experimental spectrum.

Figures 3 and S10 show the fluorescence spectra of the monomers and complexes calculated at different levels of environment treatment. Although all the transition energies are overestimated, in the fluorescence we can also see the effect of the polarizable environment combined with geometric distortion. Note that these are ensemble spectra obtained by summing the Gaussian-broadened spectra of the individual $S_1 \rightarrow S_0$ transitions in the monomers and complexes. Therefore, multiple emission peaks originate from emitters of different structures, rather than from different electronic transitions in the same emitter, in accordance with Kasha's rule.

The fluorescence of B3PYMPM [Figure 3(*a*)] originates from the low-intensity $S_1 \rightarrow S_0$ transition. The calculated dual fluorescence peaks of B3PYMPM (a relatively intense peak at ~310–320 nm and a weak peak at ~350 nm) cannot be assigned to vibronic transitions because the distance between the peaks is too large and does not correspond to any skeletal vibrations. The low-intensity emission band at ~350 nm originates from chromophores whose lowest transition is n–π* (HOMO-4→LUMO), while the more intense emission at ~300 nm comes from the lowest π–π* (HOMO→LUMO) transition. Structures whose lowest transition is π–π* are more conjugated, while in structures with the lowest n–π* transition the conjugation is broken.

The fluorescence of CBP [Figure 3(*b*)] originates from the intense $S_1 \rightarrow S_0$ transition. The calculated fluorescence spectrum of CBP also consists of two bands, a relatively long-wavelength one at ~340 nm and a blue-shifted one at ~300 nm. In this case, the difference in the structures responsible for these two bands is clearly visible: the structures with a planar biphenyl moiety give intense emission at ~340 nm, while the twisted ones give weak emission at ~300 nm.

In the fluorescence spectra of the complexes [Figure 3(*c*)], the dual peaks originate from intense local (CBP) and weak charge-transfer exciplex transitions.

No phosphorescence spectral data are available for B3PYMPM. The low-temperature emission spectra of CBP[1] consist of both fluorescence and phosphorescence bands, both of which have a distinct vibronic structure. The low-temperature emission of the co-deposited films is also due to the CBP phosphorescence. The calculated phosphorescence spectra are shown in Figure S11.

Calculation of the vibronic spectral shape of the studied molecules was beyond the scope of our work. Although molecular dynamic trajectories cannot mimic the vibronic structure of the bands, our spectra calculated using the MM and EFP environment partially retain some structure. The position of the CBP emission band agrees with experiment, and the phosphorescence band of the complexes originates from the local $T_1 \rightarrow S_0$ transition in CBP.

In general, the structural inhomogeneity of amorphous samples has a greater effect on the position and shape of spectral bands. The effect of an inhomogeneous polarizable environment is pronounced only in the case of charge transfer exciplexes.

Our calculations showed that structural inhomogeneity in an amorphous sample affects the spectra more strongly than the

polarizable environment. The inhomogeneous polarizable environment has the most pronounced effect on the charge transfer states in exciplexes. The modified QM/EFP model proved to be the most accurate environment model for describing the spectra of amorphous organic semiconductor layers. Therefore, it can be recommended for simulating the absorption and emission spectra of amorphous organic materials.

This work was supported by the Russian Science Foundation (grant no. 23-23-00429). The calculations were performed using the computational facilities of the Joint Supercomputer Center of the Russian Academy of Sciences and the University Cluster of MEPhI.

Online Supplementary Materials

Supplementary data associated with this article can be found in the online version at doi: 10.71267/mencom.7635.

References

1 Y.-S. Park, W.-I. Jeong and J.-J. Kim, *J. Appl. Phys.*, 2011, **110**, 124519; https://doi.org/10.1063/1.3672836.
2 V. Cherpak, P. Stakhira, B. Minaev, G. Baryshnikov, E. Stromylo, I. Helzhynskyy, M. Chapran, D. Volyniuk, Z. Hotra, A. Dabuliene, A. Tomkeviciene, L. Voznyak and J. V. Grazulevicius, *ACS Appl. Mater. Interfaces*, 2015, **7**, 1219; https://doi.org/10.1021/am507050g.
3 H.-B. Kim, D. Kim and J.-J. Kim, in *Highly Efficient OLEDs: Materials Based on Thermally Activated Delayed Fluorescence*, ed. H. Yersin, Wiley-VCH, Weinheim, 2018, pp. 331–376; https://doi.org/10.1002/9783527691722.ch10.
4 B. Chen, X. H. Zhang, X. Q. Lin, H. L. Kwong, N. B. Wong, C. S. Lee, W. A. Gambling and S. T. Lee, *Synth. Met.*, 2001, **118**, 193; https://doi.org/10.1016/S0379-6779(00)00278-2.
5 M. Castellani and D. Berner, *J. Appl. Phys.*, 2007, **102**, 024509; https://doi.org/10.1063/1.2757204.
6 A. E. Masunov, D. Anderson, A. Ya. Freidzon and A. A. Bagaturyants, *J. Phys. Chem. A*, 2015, **119**, 6807; https://doi.org/10.1021/acs.jpca.5b03877.
7 B. Zhang and Z. Xie, *Front. Chem.*, 2019, **7**, 306; https://doi.org/10.3389/fchem.2019.00306.
8 A. Freidzon, N. Dubinets and A. Bagaturyants, *J. Phys. Chem. A*, 2022, **126**, 2111; https://doi.org/10.1021/acs.jpca.1c10386.
9 A. Warshel and M. Levitt, *J. Mol. Biol.*, 1976, **103**, 227; https://doi.org/10.1016/0022-2836(76)90311-9.
10 W. D. Cornell, P. Cieplak, C. I. Bayly, I. R. Gould, K. M. Merz, D. M. Ferguson, D. C. Spellmeyer, T. Fox, J. W. Caldwell and P. A. Kollman, *J. Am. Chem. Soc.*, 1995, **117**, 5179; https://doi.org/10.1021/ja00124a002.
11 J. Gao, *Acc. Chem. Res.*, 1996, **29**, 298; https://doi.org/10.1021/ar950140r.
12 M. S. Gordon, L. Slipchenko, H. Li and J. H. Jensen, in *Annual Reports in Computational Chemistry*, eds. D. C. Spellmeyer and R. A. Wheeler, Elsevier, Amsterdam, 2007, vol. 3, pp. 177–193; https://doi.org/10.1016/S1574-1400(07)03010-1.
13 L. V. Slipchenko and P. K. Gurunathan, in *Fragmentation: Toward Accurate Calculations on Complex Molecular Systems*, ed. M. S. Gordon, Wiley, Hoboken, NJ, 2017, pp. 183–208; https://doi.org/10.1002/9781119129271.ch6.
14 A. V. Odinokov, N. O. Dubinets and A. A. Bagaturyants, *J. Comput. Chem.*, 2018, **39**, 807; https://doi.org/10.1002/jcc.25149.
15 N. Dubinets and L. V. Slipchenko, *J. Phys. Chem. A*, 2017, **121**, 5301; https://doi.org/10.1021/acs.jpca.7b01701.
16 A. D. Becke, *J. Chem. Phys.*, 1993, **98**, 1372; https://doi.org/10.1063/1.464304.
17 A. Schäfer, H. Horn and R. Ahlrichs, *J. Chem. Phys.*, 1992, **97**, 2571; https://doi.org/10.1063/1.463096.
18 F. Weigend and R. Ahlrichs, *Phys. Chem. Chem. Phys.*, 2005, **7**, 3297; https://doi.org/10.1039/B508541A.
19 F. Neese, *Wiley Interdiscip. Rev.: Comput. Mol. Sci.*, 2012, **2**, 73; https://doi.org/10.1002/wcms.81.
20 F. Neese, *Wiley Interdiscip. Rev.: Comput. Mol. Sci.*, 2018, **8**, e1327; https://doi.org/10.1002/wcms.1327.
21 G. M. J. Barca, C. Bertoni, L. Carrington, D. Datta, N. De Silva, J. E. Deustua, D. G. Fedorov, J. R. Gour, A. O. Gunina, E. Guidez, T. Harville, S. Irle, J. Ivanic, K. Kowalski, S. S. Leang, H. Li, W. Li, J. J. Lutz, I. Magoulas, J. Mato, V. Mironov, H. Nakata, B. Q. Pham, P. Piecuch, D. Poole, S. R. Pruitt, A. P. Rendell, L. B. Roskop, K. Ruedenberg, T. Sattasathuchana, M. W. Schmidt, J. Shen, L. Slipchenko, M. Sosonkina, V. Sundriyal, A. Tiwari, J. L. Galvez Vallejo, B. Westheimer, M. Włoch, P. Xu, F. Zahariev and M. S. Gordon, *J. Chem. Phys.*, 2020, **152**, 154102; https://doi.org/10.1063/5.0005188.
22 M. J. Abraham, T. Murtola, R. Schulz, S. Páll, J. C. Smith, B. Hess and E. Lindahl, *SoftwareX*, 2015, **1–2**, 19; https://doi.org/10.1016/j.softx.2015.06.001.
23 W. L. Jorgensen and J. Tirado-Rives, *J. Am. Chem. Soc.*, 1988, **110**, 1657; https://doi.org/10.1021/ja00214a001.
24 W. L. Jorgensen, D. S. Maxwell and J. Tirado-Rives, *J. Am. Chem. Soc.*, 1996, **118**, 11225; https://doi.org/10.1021/ja9621760.

Received: 3rd October 2024; Com. 24/7635